

## The influence of blast furnace slag content on the mechanical and durability properties of raw perlite-based geopolymer mortars

DOI:10.36909/jer.11225

Serhat Çelikten\*

Department of Civil Engineering, Nevsehir Hacı Bektaş Veli University, Nevsehir, 50300, Turkey.

\*Email: scelikten@nevsehir.edu.tr; Corresponding Author.

### ABSTRACT

In this work, 21 different raw perlite (RP) -based geopolymer mortars (RPGMs) were manufactured. Blast furnace slag (BFS) was replaced by RP in 7 different proportions with respect to the CaO/SiO<sub>2</sub> oxide ratio of RP and BFS mixture in the RPGMs. Sodium hydroxide (NaOH= 5, 10, and 15 M) was used as alkaline medium for geopolymer synthesis in the RPGMs. The ultrasound pulse velocity ( $U_{pv}$ ), flexural strength ( $f_{fs}$ ) and compressive strength ( $f_{cs}$ ), water absorption, acid and sulfate durability of the RPGMs are investigated. The test results revealed that the BFS improved the mechanical properties of RPGMs for the low and medium alkaline medium of 5M and 10M, respectively. On the other hand, BFS had negative effect on the mechanical properties of RPGMs produced at a high alkaline medium of 15M. Moreover, the BFS improved the acid and sulfate durability of the RPGMs.

**Key words:** perlite; blast furnace slag; geopolymer; mechanical properties; durability.

## INTRODUCTION

Geopolymers are inorganic polymers synthesized by polymerization of aluminosilicate precursors with alkaline solutions (Ranjbar et al., 2016). The solutions dissolve and release the tetrahedral units of  $[AlO_4]$  and  $[SiO_4]$ , and these units were linked to the polymeric precursors by sharing oxygen atoms to form the amorphous geopolymers (Timakul et al., 2016). Any materials which are rich in amorphous Al and Si can be a potential source for geopolymer precursors (Temuujin et al., 2013; Kaya, 2021; Yurt & Emiroğlu, 2020). Based on the reaction mechanisms of the precursors, two types of bond systems can be classified (Gao et al., 2017). One is the (Si + Ca) system, the major reaction product is a C-A-S-H type gel as the main reaction product with a low Ca/Si ratio and a high Al incorporation (Brough & Atkinson, 2002). The other is the (Si + Al) system, including primarily N-A-S-H type gels within three-dimensional networks (Li et al., 2010). Due to their differences in gel characteristics and reaction mechanisms, both systems exhibit dissimilar behaviors (Gao et al., 2017). These systems can be synthesized together to achieve higher strength, better durability properties, and a promising future for the application of the geopolymers (Aydın, 2013 & Tharrini & Ramasamy, 2016 & Praveen Kumar et al., 2019 & Çelikten et al., 2019).

Perlite is an igneous rock formed after the cooling of volcanic eruptions, which colors vary from gray to black (de Oliveira et al., 2019). Due to its high amorphous Si and Al content, raw perlite in powder form (RP) can be considered as a precursor material for low-Ca geopolymer synthesis (Çelikten & Isikdag, 2020). However, there are few studies performed on the potential geopolymer production with RP (Çelikten & Isikdag, 2020 & Taxiarchou et al., 2013 & Erdogan, 2015). Besides, these previous works focused on the mechanical properties of RP-based geopolymers and also, RP was used as the sole precursor for geopolymer production. On the other hand, the durability properties of RP-based

geopolymers and the properties of geopolymers synthesized from binary or ternary mixtures of RP and high-Ca precursors still need to be investigated.

As stated by the current studies, there is little information in the literature on RP-based geopolymers. Moreover, contrasting with previous studies that mainly concentrate on the mechanical properties of RP-based geopolymer mortars (RPGMs), the current study evaluates their durability performance in the acid or sulfate environment. In this work, RPGMs were prepared to investigate the mechanical and durability properties of the products. The blast furnace slag (BFS) was substituted by RP in seven different proportions in accordance with the total CaO/SiO<sub>2</sub> oxides available in the RP and BFS. The NaOH was employed for the production of RPGMs as the sole alkaline activator with three different molarities. This way, the changes in the properties of the RPGMs by the molarity of NaOH, were examined, and the role of BFS in these changes was investigated.

## EXPERIMENTAL STUDY

Raw perlite in powder form (RP) from Genper Mining Industry Trade Co., Kütahya Province, Western Turkey, was employed as the main precursor material for the RP-based geopolymer mortars (RPGMs). Blast furnace slag (BFS) was provided from Karçimsa Cement Industry located in Karabük Province, Northern Turkey. The BFS was used in the RPGMs as partial replacement precursor material by the RP. The chemical compositions of the precursor materials (RP and BFS) are given in Table 1. The specific gravities of RP and BFS were 2.54 and 2.86, respectively. Besides, the blaine specific surface areas of RP and BFS were about 3850 and 4000 cm<sup>2</sup>/g, respectively. The NaOH was in solid form with >96% purity but was used in the RPGMs as the sole alkaline activator after dissolving in water to obtain the desired molarities of 5, 10, and 15 Molar (M). Standard sand identified by CEN

(Committee of European Norms) in the EN 196-1 was used for the production of the RPGMs. The grading of the sand is given in Table 2.

**Table 1** Chemical compositions of precursors.

Oxide (%)	SiO <sub>2</sub>	CaO	Al <sub>2</sub> O <sub>3</sub>	Fe <sub>2</sub> O <sub>3</sub>	SO <sub>3</sub>	Na <sub>2</sub> O	K <sub>2</sub> O	MgO	Loss of Ignition
Blast furnace slag	32.47	32.45	9.94	1.25	0.82	0.31	0.85	9.31	0.46
Perlite	71.36	0.96	13.08	0.78	0.12	3.21	5.42	0.12	2.12

**Table 2** The Grading of Sand.

Sieve Size (mm)	2.0	1.6	1.0	0.50	0.16	0.08
Cumulative Percentage	0	7	32	68	87	99

A total of 21 RPGM mixtures were prepared by varying the RP, BFS, and NaOH contents. The water and sand contents were kept constant to investigate the effect of the activator and precursor (RP and BFS) contents. The proportion of water to total precursor content (RP+BFS) ratio was 1:2 and the proportion of sand to precursor content was 3:1. The molarity variations of NaOH in the mixtures were 5, 10, and 15M. The BFS was replaced by RP according to the total CaO/SiO<sub>2</sub> oxide ratio of these precursors. The CaO/SiO<sub>2</sub> ratio of the precursors was designed as the increasing rate from 0.01 (RP as sole precursor) to 0.30. The mixture proportions of RPGMs for the three-cell mortar mould are shown in Table 3. As seen on the table, the RPGM mixtures were coded as the molarity of NaOH and the CaO/SiO<sub>2</sub> ratio of the precursors, respectively. Besides, the mixing procedures of RPGMs involved the following steps. The NaOH solution and RP+BFS mixture were put in the mixing bowl of Hobart mixer and mixed at 140 rpm (revolutions per minute) for 30 seconds. After the first 30 seconds, the sand was poured into the bowl in 30 seconds during mixing. Then, the mixture was mixed at 280 rpm for 30 seconds. After that, the mixture was held waiting in the bowl at a non-operating state for 90 seconds. Then, the mixture was mixed at 280 rpm for 60 seconds. Finally, the mixture was cast into 4×4×16 cm molds after waiting 15 seconds in compliance with the EN 196-1 standard. Immediately after casting, the RPGMs

were subjected to heat-curing in an oven at 100 °C without being covered for 24 hours. Twenty-four 4×4×16 cm mortar specimens were obtained from each mixture to use the mechanical and durability tests. Three RPGM specimens were employed for each test and the final test results were obtained from averaging of three values obtained from the three specimens.

**Table 3** Mix proportions of the mortars

Serial Code	Mixture Code	RP (g)	BFS (g)	NaOH (g)	Sand (g)	Water (g)	CaO/SiO <sub>2</sub> Ratio of Precursors
5M	5M-0.01	450	0	45	1350	225	0.01
	5M-0.05	414	36	45	1350	225	0.05
	5M-0.10	369	81	45	1350	225	0.10
	5M-0.15	333	117	45	1350	225	0.15
	5M-0.20	297	153	45	1350	225	0.20
	5M-0.25	266	184	45	1350	225	0.25
	5M-0.30	239	211	45	1350	225	0.30
10M	10M-0.01	450	0	90	1350	225	0.01
	10M-0.05	414	36	90	1350	225	0.05
	10M-0.10	369	81	90	1350	225	0.10
	10M-0.15	333	117	90	1350	225	0.15
	10M-0.20	297	153	90	1350	225	0.20
	10M-0.25	266	184	90	1350	225	0.25
	10M-0.30	239	211	90	1350	225	0.30
15M	15M-0.01	450	0	135	1350	225	0.01
	15M-0.05	414	36	135	1350	225	0.05
	15M-0.10	369	81	135	1350	225	0.10
	15M-0.15	333	117	135	1350	225	0.15
	15M-0.20	297	153	135	1350	225	0.20
	15M-0.25	266	184	135	1350	225	0.25
	15M-0.30	239	211	135	1350	225	0.30

The ultrasonic pulse velocity ( $U_{pv}$ ), flexural strength ( $f_{fs}$ ), compressive strength ( $f_{cs}$ ), and water absorption tests were performed on the RPGMs after 24 hours from the heat-curing process. The  $U_{pv}$  tests were conducted according to ASTM C597-16. The accuracy of  $U_{pv}$  test was 0.10 s. The  $f_{cs}$  and  $f_{fs}$  tests were executed with a universal testing machine in compliance with TS EN 1015-11. The  $f_{fs}$  tests were conducted on the RPGMs in center-point

(i.e. three-point) loading conditions. The semi-prisms were broken after the  $f_{fs}$  tests were used for the  $f_{cs}$  tests. The  $f_{cs}$  tests were conducted by placing 4×4 cm thin steel plates on the both top and bottom of broken specimens. The water absorption test was performed on the RPGMs according to ASTM C 642-06 standard. Besides, six specimens for each RPGM mixture were immersed in HCl solution (pH=2), 5% Na<sub>2</sub>SO<sub>4</sub>, and 5% MgSO<sub>4</sub> solutions for 90 and 180 days, separately. The  $f_{cs}$  test was conducted on these specimens after immersion in the solutions. Finally, the residual  $f_{cs}$  values of the RPGMs were calculated with the following equation:

$$\text{Residual } f_{cs} (\%) = [(f_{csi} - f_{csf}) / f_{csi}] \times 100 \quad (1)$$

Where,  $f_{csi}/f_{csf}$  are the  $f_{cs}$  of the RPGM specimens unexposed/exposed to acid or sulfate, solutions, respectively.

## RESULTS AND DISCUSSION

Figure 1 and Table 4 reports the  $U_{pv}$  results of the RPGMs. The  $U_{pv}$  of RPGMs was affected by the amount of BFS and molarity of NaOH, significantly. The  $U_{pv}$  values of RPGMs made with 5M, 10M and 15M NaOH solution were in the range of 2.2–3.5 km/sec., 2.6–3.4 km/sec. and 2.6–2.9 km/sec., respectively. It was clear that an increase in NaOH content led to improved  $U_{pv}$  for RPGMs made with only RP as a precursor (CaO/SiO<sub>2</sub> ratio is 0.01). The observed improvement in the  $U_{pv}$  of these RPGMs by including higher NaOH can be attributed to the development a more compact microstructure and better activation of RP at high alkali concentration as reported in previous studies (Çelikten & Isikdag, 2020 & Erdogan, 2015). The BFS caused to increase the  $U_{pv}$  of RPGMs. Moreover, the BFS content became more effective as the decreasing NaOH concentration. The  $U_{pv}$  of RPGMs was enhanced up to 59%, 30%, and 7.5% by increasing CaO/SiO<sub>2</sub>ratio of the precursors (RP and BFS) from 0.01 to 0.3 at 5M, 10M, and 15M alkaline medium, respectively. It was

previously reported that  $U_{pv}$  of mortars decreased with porosity (Mendes et al., 2020 & Lafhaj & Goueygou, 2009). Also, it was indicated that the geopolymers made with precursors having low CaO/SiO<sub>2</sub> ratio have more porous microstructure than the geopolymers produced with a high CaO/SiO<sub>2</sub> ratio (Luna Galiano et al., 2016). These results were compatible with the decrease in the  $U_{pv}$  of RPGMs as increasing BFS or CaO/SiO<sub>2</sub> ratio.

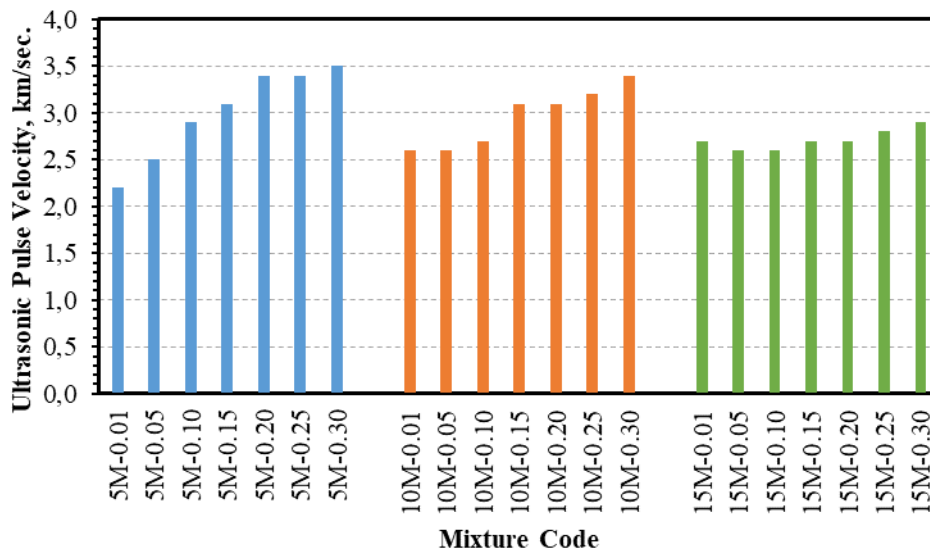


**Figure 1** Ultrasonic pulse velocity results of RPGMs.

The  $f_{fs}$  results in the various RPGMs are plotted in Figure 2 and Table 4 with varying CaO/SiO<sub>2</sub> ratios and NaOH concentrations. From the results, it could be observed that both alkali content of NaOH solution and replacement level of BFS by RP had an important influence on the  $f_{fs}$  development of the RPGMs. The  $f_{fs}$  values of RPGMs in the series of 5M, 10M, and 15M NaOH solution were in the intervals of 2.5-3.4 MPa, 4.7-5.1 MPa, and 3.0-5.9 MPa, respectively. The  $f_{fs}$  of RPGMs enhanced as increasing molarity of NaOH from 5M to 10M, significantly. The enhancement was more distinct for the RPGMs having CaO/SiO<sub>2</sub> ratios of 0.01 and 0.05. On the other hand,  $f_{fs}$  values of the RPGMs made with CaO/SiO<sub>2</sub> ratio of above 0.1 decreased as increasing the molarity of NaOH from 10M to 15M. The  $f_{fs}$  values of the 15M-0.25 and 15M-0.30 RPGMs were almost 38% lower than the

10M-0.25 and 10M-0.30 RPGMs. These results indicate that the activation of BFS was negatively influenced by the higher NaOH concentration than 10M. It can be said that the RP showed better activation in a high alkaline medium with respect to the BFS. Besides, the highest  $f_{fs}$  of 5.9 MPa was achieved for the 15M-0.01 mortars in all the RPGMs.

**Table 4** Test results of the RPGMs.

Mix code	$U_{pv}$ (km/sec.)	$f_{fs}$ (MPa)	$f_{cs}$ (MPa)	Water Abs. (%)	$f_{cs}$ after 90 days HCl immersion (MPa)	$f_{cs}$ after 180 days HCl immersion (MPa)	$f_{cs}$ after 90 days Na <sub>2</sub> SO <sub>4</sub> immersion (MPa)	$f_{cs}$ after 180 days Na <sub>2</sub> SO <sub>4</sub> immersion (MPa)	$f_{cs}$ after 90 days MgSO <sub>4</sub> immersion (MPa)	$f_{cs}$ after 180 days MgSO <sub>4</sub> immersion (MPa)
5M-0.01	2.2	2.5	11.6	11.3	4.0	3.6	4.2	3.7	4.1	3.4
5M-0.05	2.5	2.6	12.2	11.0	4.3	3.8	4.5	3.9	4.3	3.9
5M-0.10	2.9	3.3	15.3	10.4	5.8	4.7	6.1	5.0	5.7	4.8
5M-0.15	3.1	3.4	17.4	9.6	8.0	7.1	8.8	7.4	7.7	6.9
5M-0.20	3.4	3.4	18.8	8.8	9.3	8.4	9.5	8.7	9.2	8.4
5M-0.25	3.4	3.2	20.1	8.1	10.4	9.1	10.5	9.4	10.3	9.4
5M-0.30	3.5	3.4	22.5	7.6	11.7	10.3	12.2	10.6	11.5	10.1
10M-0.01	2.6	5.1	20.8	10.9	5.1	4.2	5.4	4.5	4.9	4.1
10M-0.05	2.6	4.8	21.3	10.7	5.0	4.1	5.8	4.8	5.1	4.3
10M-0.10	2.7	4.7	21.9	10.3	7.3	6.1	7.9	6.6	7.1	5.9
10M-0.15	3.1	4.9	22.5	9.3	7.5	6.3	10.5	8.8	8.7	7.3
10M-0.20	3.1	4.7	22.6	8.9	9.7	8.1	11.2	9.4	9.6	8.0
10M-0.25	3.2	5.0	24.3	8.3	10.3	8.6	12.6	10.5	10.9	9.1
10M-0.30	3.4	4.8	24.8	7.8	11.0	9.2	13.0	10.8	11.1	9.3
15M-0.01	2.7	5.9	23.6	10.2	5.3	4.1	5.6	4.3	5.2	4.1
15M-0.05	2.6	5.2	23.4	10.0	5.2	4.0	5.5	4.2	5.1	4.2
15M-0.10	2.6	4.7	23.0	9.8	6.4	5.3	6.7	5.6	6.3	5.3
15M-0.15	2.7	4.4	21.2	9.7	6.5	5.7	6.9	6.0	6.6	5.8
15M-0.20	2.7	3.9	20.8	9.4	6.8	6.0	7.1	6.3	7.0	5.8
15M-0.25	2.8	3.1	18.9	9.0	7.1	6.2	7.5	6.5	7.0	5.9
15M-0.30	2.9	3.0	18.3	8.7	7.6	6.1	7.9	6.4	7.7	6.1



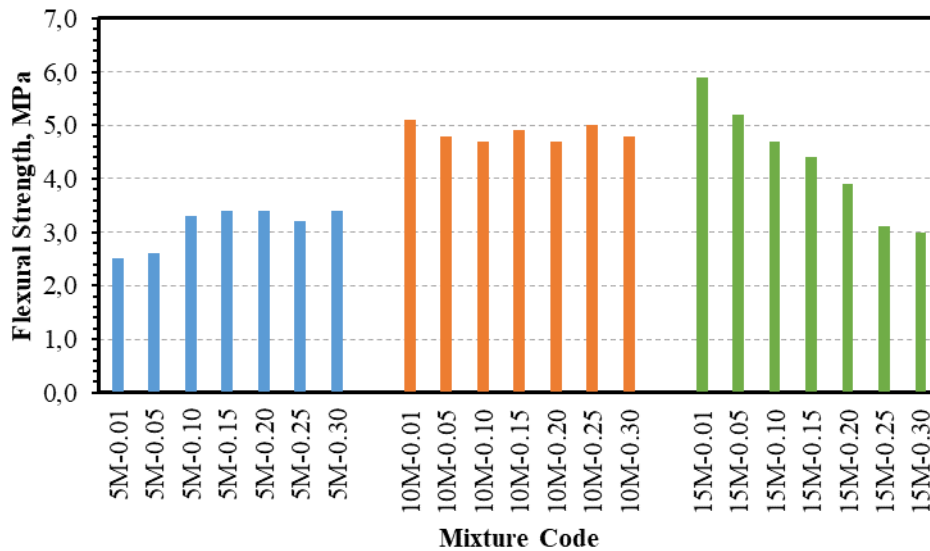


**Figure 2** Flexural strength results of RPGMs.

Figure 3 and Table 4 show the  $f_{cs}$  test results of the RPGMs. The highest  $f_{cs}$  of 24.8 MPa was recorded for 10M-0.30 RPGMs. The  $f_{cs}$  values of the RPGMs made by using RP as the sole precursor ( $\text{CaO}/\text{SiO}_2=0.01$ ) improved by increasing NaOH content. The  $f_{cs}$  increase was 79% and 13% in these RPGMs from 5M to 10M and from 10M to 15M, respectively. With increasing concentration of NaOH in the RPGMs, the solubilities of amorphous Si and Al in RP also increased as stated in previous works for fly ash (Çelikten & Isikdag, 2020) and calcined clay (El Hafid et al., 2017) as another low Ca precursors. The  $f_{cs}$  values of the RPGMs significantly increased by increasing the  $\text{CaO}/\text{SiO}_2$  ratio or the BFS content for the 5M NaOH medium. On the other hand, the  $f_{cs}$  values of RPGMs decreased as increasing the BFS content at 15M alkaline medium. These results indicate that the 15M NaOH content negatively influenced the dissolution of Si and Al species from the BFS. The lower dissolution of these species can be attributed to the excessive  $\text{OH}^-$  (Part et al., 2015 & Cho et al., 2017) or excessive  $\text{Na}^+$  (Sun et al., 2018) adsorbed on the surface of fly ash particles as stated for fly ash-based geopolymers in the previous works. The optimum alkaline concentration varies from one precursor to another due to their different solubility and degree of amorphousness. For example, in previous works, 12M NaOH was reported as appropriate

molarity for ceramic sanitaryware waste-based geopolymers (Atabey & Ozturk, 2020) and 16M for expanded perlite-based geopolymer mortars (Çelikten & Isikdag, 2020). In the present work, BFS exhibits better activation than the RP in a low alkaline medium. Additionally, the  $f_{fs}/f_{cs}$  ratios of the RPGMs were gradually decreased as increasing BFS content. The ratio was 0.21, 0.24 and 0.25 for the 5M-0.01, 10M-0.01 and, 15M-0.01 RPGMs, respectively. On the other hand, the 5M-0.30, 10M-0.30 and, 15M-0.30 RPGMs had the  $f_{fs}/f_{cs}$  ratios of 0.15, 0.19, and 0.16, respectively. The reason for decrease in the ratio with BFS inclusion can be attributed to the sensitivity of BFS to the heat-curing process.

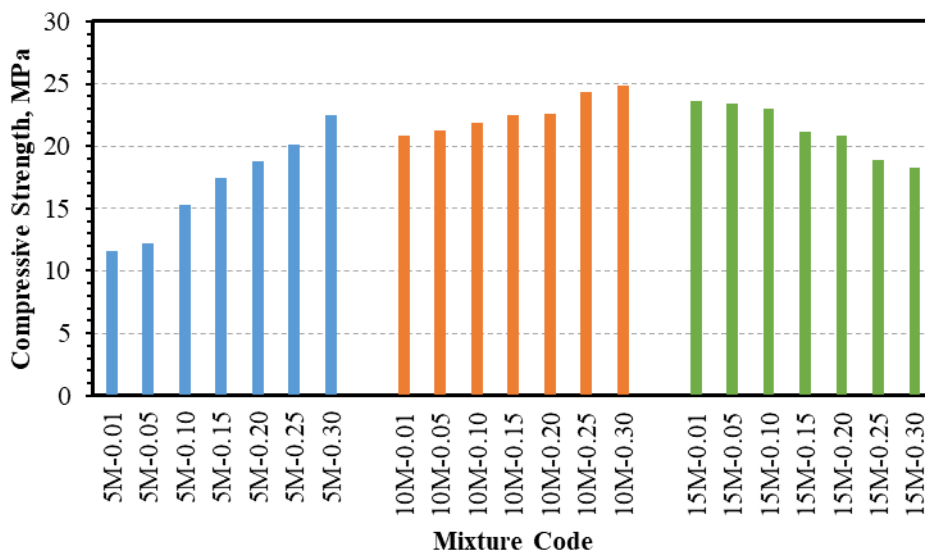


**Figure 3** Compressive strength results of RPGMs.

The influence of CaO/SiO<sub>2</sub> ratio and NaOH content on the water absorption of RPGMs is shown in Figure 4 and Table 4. It can be seen from this figure that the water absorption capacity of RPGMs increased as increasing the CaO/SiO<sub>2</sub> ratio independently of the NaOH molarity. Besides, the water absorption capacity of the RPGMs which have CaO/SiO<sub>2</sub> ratio lower than 0.15 decreased gradually as increasing the molarity of NaOH. However, the capacity of the RPGMs designed with the CaO/SiO<sub>2</sub> ratios of 0.20, 0.25, and 0.30 increased as increasing NaOH molarity. These results were compatible with the  $U_{pv}$  results. These results are likely to be related to the better activation of BFS at low NaOH molarity resulting

in low pore volume for the RPGMs. In a previous work (Yusuf et al., 2014), it was reported that the increase in the Ca content by the inclusion of BFS in the low Ca geopolymer system (ultrafine palm oil fuel ash-based geopolymer was studied in the previous work) caused to increase the density of the products through pore filling effect. As stated in other previous studies, the utilization of BFS by fly ash in the low Ca geopolymer systems, gave a decrease in total porosity (Provis et al., 2012) and caused to decrease in the water absorption capacity (Sarıdemir & Çelikten, 2020). In the present work, the  $U_{pv}$  and water absorption results indicate the filling effect of BFS in the RPGMs as stated in the previous works.

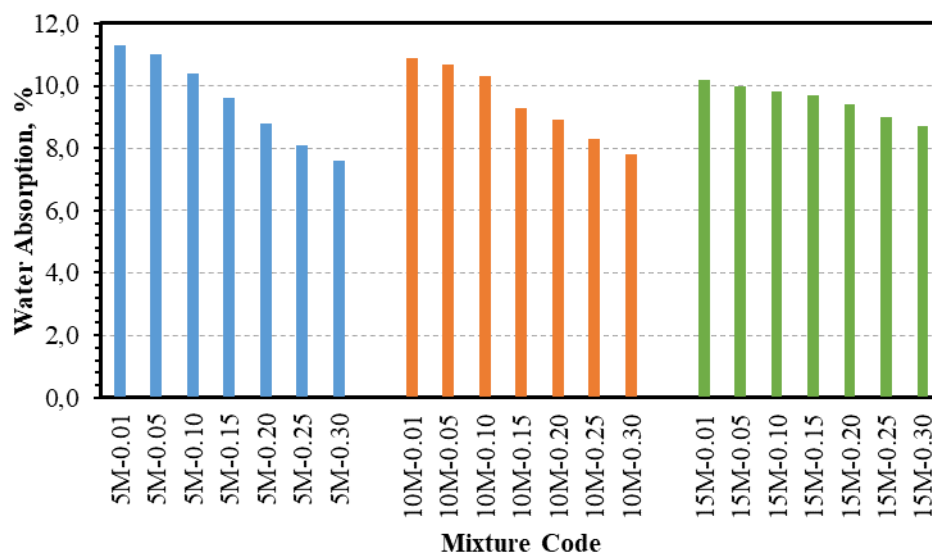


**Figure 4** Water absorption results of RPGMs.

The acid resistance of the RPGMs was evaluated based on the change in  $f_{cs}$  of mortar specimens after exposure to HCl solution (pH=2) for 90 and 180 days, separately. Figure 5 and Table 4 show the residual  $f_{cs}$  and final  $f_{cs}$  results of RPGMs after immersion of the HCl solution, respectively. The residual  $f_{cs}$  of the 5M-0.01 RPGMs decreased to about 34.5% and 31% for 90 and 180 days' immersion periods, respectively. The inclusion of BFS increased the residual  $f_{cs}$  of the RPGMs. The highest residual  $f_{cs}$  values were observed on the 5M-0.30 as 52% and 45.8% after immersion for 90 and 180 days, respectively. The improved durability of the RPGMs to the acid environment with the BFS content can be attributed to

the difficult diffusion of  $H^+$  ions to the inner structure of the mortars. The difficulty in the diffusion of the ions may be originated from the change in the pore structure of the RPGMs with BFS content as supported by  $U_{pv}$  and water absorption results. Besides, the residual  $f_{cs}$  of the RPGMs decreased as increasing the molarity of NaOH due to the lower activation of BFS in high molarities. The lowest residual  $f_{cs}$  values were observed on the 15M-0.01 and 15M-0.05 RPGMs. On the other hand, the  $f_{cs}$  values of these RPGMs were still higher than the 5M-0.01 and 5M-0.05 RPGMs after immersion to the HCl solution.

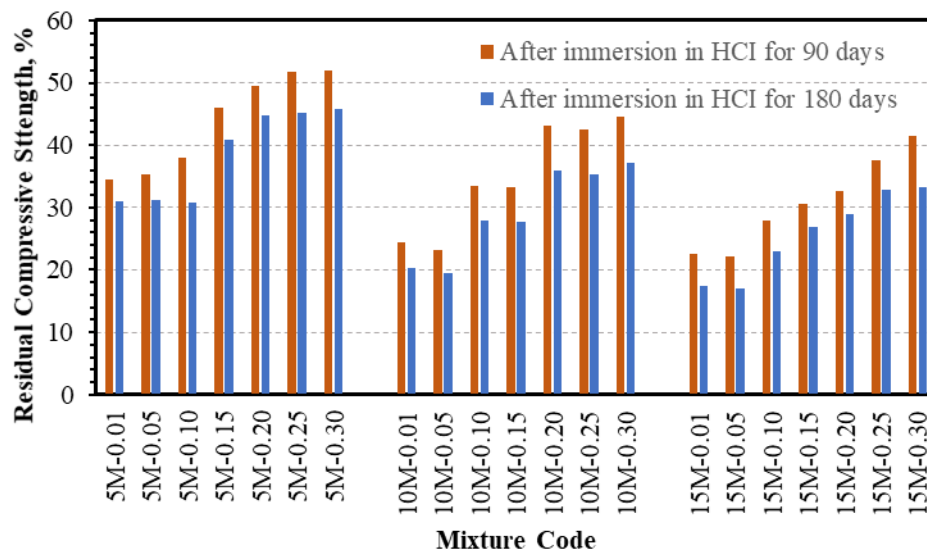


**Figure 5** Residual compressive strengths of RPGMs after exposure to acid.

The residual  $f_{cs}$  and final  $f_{cs}$  values of the RPGMs after exposure to 5%  $Na_2SO_4$  solution for 90 and 180 days are given in Figure 6 and Table 4, respectively. The residual  $f_{cs}$  values were in the ranges of 36-55%, 26-53%, and 23-43% for the RPGMs in the series of 5M, 10M, and 15M after exposure to  $Na_2SO_4$  solution for 90 days. After immersion for 180 days, the values were decreased between 4% and 9% with respect to the proportions calculated after 90 days' immersion. The highest residual  $f_{cs}$  values were observed on the RPGMs manufactured as the CaO/SiO<sub>2</sub> ratio of 0.30 in all the series. The highest  $f_{cs}$  values of 13.0 and 10.8 MPa were achieved on the 10M-0.30 RPGMs after exposure to  $Na_2SO_4$  solution for 90 and 180 days, respectively. Besides, an increase in the molarity of NaOH had a negative influence on the

residual  $f_{cs}$  of the RPGMs as reported for the results in the acid environment. The lowest residual  $f_{cs}$  of 17.9% was calculated for the 15M-0.05 RPGMs after exposure to  $\text{Na}_2\text{SO}_4$  solution for 180 days. Additionally, the residual  $f_{cs}$  values of the RPGMs after exposure to  $\text{Na}_2\text{SO}_4$  solution were slightly higher than the values after exposure to HCl solution.

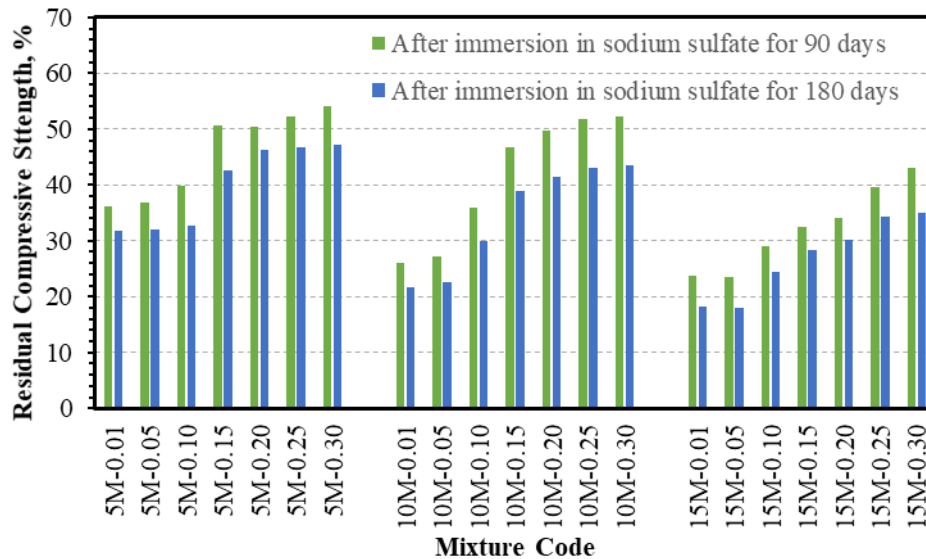


**Figure 6** Residual compressive strengths of RPGMs after exposure to  $\text{Na}_2\text{SO}_4$ .

The residual  $f_{cs}$  percentages and final  $f_{cs}$  values of the RPGMs after immersion in 5%  $\text{MgSO}_4$  solution for 90 and 180 days are given in Figure 7 and Table 4, respectively. While the lowest residual  $f_{cs}$  of 17.4% was seen on the 15M-0.01 RPGMs after immersion to the solution for 180 days, the highest  $f_{cs}$  of 46.8% was observed on the 5M-0.25 RPGMs at the same condition. As seen on the figure, the residual  $f_{cs}$  percentages of the RPGMs increased as increasing BFS content as observed after exposure to HCl and  $\text{Na}_2\text{SO}_4$  solutions. The better activation of BFS at lower NaOH content also increased the residual  $f_{cs}$  percentages of the RPGMs in the series of 5M with respect to the other series. Besides, the durability test results indicate that the HCl (pH=2) and 5%  $\text{MgSO}_4$  solutions had a more detrimental effect on the  $f_{cs}$  of the RPGMs than the 5%  $\text{Na}_2\text{SO}_4$  solution. The major loss in the  $f_{cs}$  of the RPGMs was noted after immersion to the acid or sulfate solutions for 90 days. The decrease in the  $f_{cs}$  values of the mortars was more limited from 90 to 180 days than the 0 to 90 days.

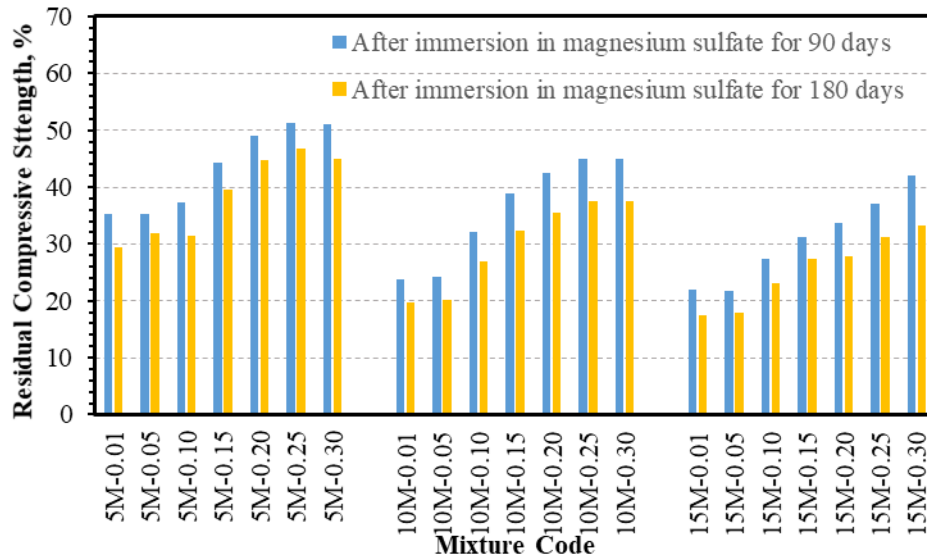


**Figure 7** Residual compressive strengths of RPGMs after exposure to  $\text{MgSO}_4$ .

## CONCLUSION

The mechanical and durability properties of blast furnace slag incorporated ground perlite-based geopolymer mortars are investigated in this study. With regard to the analysis of results obtained from this work, the following conclusions are revealed from these results:

- The optimum BFS content in the ground perlite-based geopolymer mortars is variable dependent on the molarity of NaOH. The best results in respect of mechanical and durability properties were achieved on the 10M-0.30 mortars.
- The effect of NaOH concentration changed with the precursor combination (CaO/SiO<sub>2</sub> ratio). The mechanical properties of ground perlite-based geopolymer mortars improved as increasing NaOH molarity. The optimum NaOH molarity was determined as 10M for the blast furnace slag incorporated ground perlite-based geopolymer mortars.
- Water absorption capacity of ground perlite-based geopolymer mortars decreased as increasing the blast furnace slag content independent from the NaOH molarity. The influence of blast furnace slag was more distinct at low NaOH content.

- The flexural strength/compressive strength ratio of the ground-perlite based geopolymer mortars decreased gradually as increasing the blast furnace slag content.
- Blast furnace slag incorporation in the ground perlite-based geopolymer mortars increased the acid and sulfate durability of these mortars, significantly.
- Magnesium sulfate and hydrochloric acid had a more detrimental influence on the strength of ground perlite-based geopolymer mortars with respect to the sodium sulfate.

## REFERENCES

- ASTM C 597, 2016.** Standard Test Method for Pulse Velocity through Concrete, American Society for Testing and Materials, West Conshohocken, PA, USA.
- ASTM C 642–06, 2006.** Standard test method for density, absorption, and voids in hardened concrete, PP 1- 3, ASTM International, Pennsylvania, United States,
- Atabey, İ. İ. & Oztürk, Z. B. 2021.** Investigation of Usability of Ceramic Sanitaryware Wastes in Geopolymer Mortar Production. *International Journal of Engineering Research and Development*. 13(1): 212-219. <https://doi.org/10.29137/umagd.782733>
- Aydın, S. 2013.** A ternary optimisation of mineral additives of alkali activated cement mortars. *Construction and Building Materials*. 43: 131-138. <https://doi.org/10.1016/j.conbuildmat.2013.02.005>
- Brough, A. R. & Atkinson, A. 2002.** Sodium silicate-based, alkali-activated slag mortars: Part I. Strength, hydration and microstructure. *Cement and Concrete Research*. 32(6): 865-879. [https://doi.org/10.1016/S0008-8846\(02\)00717-2](https://doi.org/10.1016/S0008-8846(02)00717-2)
- Celikten, S. & Isikdag, B. 2020.** Strength development of ground perlite-based geopolymer mortars. *Advances in Concrete Construction*. 9(3): 227-234.
- Çelikten, S., & Işıkdag, B. 2021.** Properties of geopolymer mortars derived from ground calcined perlite and NaOH solution. *European Journal of Environmental and Civil*

Engineering, 1-15. <https://doi.org/10.1080/19648189.2021.1879939>

**Çelikten, S., Sarıdemir, M. & Deneme, İ. Ö. 2019.** Mechanical and microstructural properties of alkali-activated slag and slag+ fly ash mortars exposed to high temperature. *Construction and Building Materials*. 217: 50-61.

<https://doi.org/10.1016/j.conbuildmat.2019.05.055>

**Cho, Y. K., Yoo, S. W., Jung, S. H., Lee, K. M. & Kwon, S. J. 2017.** Effect of Na<sub>2</sub>O content, SiO<sub>2</sub>/Na<sub>2</sub>O molar ratio, and curing conditions on the compressive strength of FA-based geopolymer. *Construction and Building Materials*. 145: 253-260.

**de Oliveira, A. G., Jandorno Jr, J. C., da Rocha, E. B. D., de Sousa, A. M. F. & da Silva, A. L. N. 2019.** Evaluation of expanded perlite behavior in PS/Perlite composites. *Applied Clay Science*. 181: 105223. <https://doi.org/10.1016/j.clay.2019.105223>

**El Hafid, K., Hajjaji, M. & El Hafid, H. 2017.** Influence of NaOH concentration on microstructure and properties of cured alkali-activated calcined clay, *Journal of Building Engineering*. 11: 158-165. <https://doi.org/10.1016/j.jobe.2017.04.012>.

**EN 196-1, 2016.** Methods of Testing Cement–Part 1: Determination of Strength, European Committee for Standardization (CEN),

**Erdogan, S. T. 2015.** Properties of ground perlite geopolymer mortars. *Journal of Materials in Civil Engineering*. 27(7): 04014210. [https://doi.org/10.1061/\(ASCE\)MT.1943-5533.0001172](https://doi.org/10.1061/(ASCE)MT.1943-5533.0001172)

**Gao, X., Yu, Q. L., Yu, R. & Brouwers, H. J. H. 2017.** Evaluation of hybrid steel fiber reinforcement in high performance geopolymer composites. *Materials and Structures*. 50(2): 165. <https://doi.org/10.1617/s11527-017-1030-x>

**Kaya, M. 2021.** The effect of silica fume and micro SiO<sub>2</sub> additive on the strength properties in kaolin based geopolymer mortars. *Niğde Ömer Halisdemir University Journal of Engineering Sciences*, 1-1. <https://doi.org/10.28948/ngumuh.886863>

**Lafhaj, Z. & Goueygou, M. 2009.** Experimental study on sound and damaged mortar: Variation of ultrasonic parameters with porosity. *Construction and Building Materials*.



23(2): 953-958. <https://doi.org/10.1016/j.conbuildmat.2008.05.012>

**Li, C., Sun, H. & Li, L. 2010.** A review: The comparison between alkali-activated slag (Si+ Ca) and metakaolin (Si+ Al) cements. *Cement and Concrete Research*. 40(9): 1341-1349. <https://doi.org/10.1016/j.cemconres.2010.03.020>

**Luna Galiano, Fernández Pereira, Y. C. & Izquierdo. M. 2016.** Contributions to the study of porosity in fly ash-based geopolymers. Relationship between degree of reaction, porosity and compressive strength, *Materiales de Construccion*. 66: 324. <https://doi.org/10.3989/mc.2016.10215>.

**Mendes, J. C., Barreto, R. R., Costa, L. C. B., Brigolini, G. J. & Peixoto, R. A. F. 2020.** Correlation Between Ultrasonic Pulse Velocity and Thermal Conductivity of Cement-Based Composites. *Journal of Nondestructive Evaluation*. 39(2). <https://doi.org/10.1007/s10921-020-00680-7>

**Part, W.K., Ramli, M. & Cheah, C.B. 2015.** An overview on the influence of various factors on the properties of geopolymer concrete derived from industrial by-products, *Construction and Building Materials*. 77: 370-395. <https://doi.org/10.1016/j.conbuildmat.2014.12.065>.

**Praveen Kumar, V. V., Prasad, N. & Dey, S. 2019.** Influence of metakaolin on strength and durability characteristics of ground granulated blast furnace slag based geopolymer concrete. *Structural Concrete*. <https://doi.org/10.1002/suco.201900415>

**Provis, J. L., Myers, R. J., White, C. E., Rose, V. & Van Deventer, J. S. 2012.** X-ray microtomography shows pore structure and tortuosity in alkali-activated binders. *Cement and Concrete Research*. 42(6): 855-864. <https://doi.org/10.1016/j.cemconres.2012.03.004>

**Ranjbar, N., Talebian, S., Mehrali, M., Kuenzel, C., Metselaar, H. S. C. & Jumaat, M. Z. 2016.** Mechanisms of interfacial bond in steel and polypropylene fiber reinforced geopolymer composites. *Composites Science and Technology*. 122: 73-81. <https://doi.org/10.1016/j.compscitech.2015.11.009>

**Sarıdemir, M. & Çelikten, S. 2020.** Investigation of fire and chemical effects on the

- properties of alkali-activated lightweight concretes produced with basaltic pumice aggregate. *Construction and Building Materials*. 260: 119969. <https://doi.org/10.1016/j.conbuildmat.2020.119969>
- Sun, Q. Zhu, H. Li, H. Zhu, H. Gao, M. 2018.** Application of response surface methodology in the optimization of fly ash geopolymer concrete. *Revista Romana de Materiale*. 48(1): 45-52. <http://solacolu.chim.upb.ro/p45-52.pdf>
- Taxiarchou, M., Pantias, D., Panagiotopoulou, C., Karalis, A. & Dedeloudis, C. 2013.** Study on the suitability of volcanic amorphous aluminosilicate rocks (perlite) for the synthesis of Geopolymer-based concrete. In *Geopolymer Binder Systems*. ASTM International. <https://doi.org/10.1520/STP156620120077>
- Temuujin, J., Rickard, W. & Van Riessen, A. 2013.** Characterization of various fly ashes for preparation of geopolymers with advanced applications. *Advanced Powder Technology*. 24(2): 495-498. <https://doi.org/10.1016/j.appt.2013.01.013>
- Thaarrini, J. & Ramasamy, V. 2016.** Properties of foundry sand, ground granulated blast furnace slag and bottom ash based geopolymers under ambient conditions. *Periodica Polytechnica Civil Engineering*. 60(2): 159-168. <https://doi.org/10.3311/PPci.8014>
- Timakul, P., Rattanaprasit, W. & Aungkavattana, P. 2016.** Improving compressive strength of fly ash-based geopolymer composites by basalt fibers addition. *Ceramics International*. 42(5): 6288-6295. <https://doi.org/10.1016/j.ceramint.2016.01.014>
- TS EN 1015-11, 2000.** Methods of test for mortar for masonry-part 11: determination of flexural and compressive strength of hardened mortar. Turkish Standards Institution, Ankara, Turkey.
- Yurt, U. & Emiroğlu, M. 2020.** The Effects of Curing Condition on Geopolymers Incorporating Zeolit. *Academic Platform Journal of Engineering and Science*. 8(2): 396-402. <https://doi.org/10.21541/apjes.688186>
- Yusuf, M. O., Johari, M. A. M., Ahmad, Z. A. & Maslehuddin, M. 2014.** Strength and microstructure of alkali-activated binary blended binder containing palm oil fuel ash and

ground blast-furnace slag. Construction and Building Materials. 52: 504-510.

<https://doi.org/10.1016/j.conbuildmat.2013.11.012>